Multi-radionuclide digital autoradiography of the intra-aortic atherosclerotic plaques using a monoclonal antibody targeting oxidized low-density lipoprotein.

Örbom, Anders; Jansson, Bo; Schiopu, Alexandru; Evans Axelsson, Susan; Nilsson, Jan; Nordin Fredrikson, Gunilla; Strand, Sven-Erik

Published in:
American journal of nuclear medicine and molecular imaging

2014

Am J Nucl Med Mol Imaging 2014;4(2):172-180
www.ajnmmi.us /ISSN:2160-8407/ajnmmi1310003

Original Article

Multi-radionuclide digital autoradiography of the intra-aortic atherosclerotic plaques using a monoclonal antibody targeting oxidized low-density lipoprotein

Anders Örbom[1], Bo Jansson[2], Alexandru Schiopu[3,4], Susan Evans-Axelsson[5], Jan Nilsson[3], Gunilla Nordin Fredrikson[3], Sven-Erik Strand[1]

[1]Department of Medical Radiation Physics, Lund University, Lund, Sweden; [2]Bioinvent International AB, Lund, Sweden; [3]Experimental Cardiovascular Research Unit, Department of Clinical Sciences, Skåne University Hospital Malmö, Lund University, Sweden; [4]Cardiology Clinic, Skåne University Hospital Malmö, Sweden; [5]Division of Urological Cancers, Department of Clinical Sciences, Skåne University Hospital Malmö, Lund University, Malmö, Sweden

Received October 21, 2013; Accepted November 27, 2013; Epub March 20, 2014; Published March 30, 2014

Abstract: The aim of this study was to use multi-radionuclide autoradiography to compare the different distributions of three radiolabelled tracers in an atherosclerotic mouse model. This method, along with immunohistochemistry, was applied to investigate the intra-aortic distribution of 2-deoxy-2-[^{18}F]fluoro-D-glucose (^{18}F-FDG), ^{131}I/^{125}I labeled anti-oxidized Low Density Lipoprotein (oxLDL), and non-binding control antibodies. Aortas were isolated from a total of 12 apoB-100/LDL receptor deficient mice 73 h post injection of radioiodine-labeled anti-oxLDL and control antibody and 1 h post injection of ^{18}F-FDG. A solid-state real-time digital autoradiography system was used to image the slide mounted aortas. Contributions from each radionuclide were separated by half-life and emission energy and the aortas were subsequently stained with Oil Red O for plaque to aorta contrast ratios. Immunohistochemical staining was performed to detect anti-oxLDL and control antibody localization. Radiolabeled anti-oxLDL showed increased total activity uptake in the aorta over control antibody and immunohistochemical analysis of plaques indicated increased binding of the specific antibody compared to control. The intra-aortic activity distribution of the anti-oxLDL antibody was however very similar to that of the control antibody although both had higher atherosclerotic plaques to aorta wall ratios than ^{18}F-FDG. Given the right choice of radionuclides, multi-radionuclide digital autoradiography can be employed to compare several tracers *ex vivo* in the same animal. The distribution of anti-oxLDL antibodies did not significantly differ from the control antibody but it did appear to have a better plaque to aorta contrast at 73 h post injection than ^{18}F-FDG at 1 h post injection.

Keywords: Autoradiography, atherosclerosis, oxidized low density lipoprotein, multi-radionuclide imaging

Introduction

Atherosclerosis is a chronic inflammatory disease that is initiated and develops as the result of an inflammatory response to accumulation of oxidized lipid and lipoproteins in the arterial wall [1]. Lipoprotein oxidation results in the formation of a number of reactive aldehydes, oxidized phospholipids and other lipid derivatives, leading to tissue damage and macrophage activation. The lesions may progress into vulnerable plaques that are prone to rupture and cause thrombosis with fatal consequences for the patient. Oxidized Low Density Lipoprotein (oxLDL) is known to promote plaque inflammation in atherosclerosis. Treatment with monoclonal antibodies (mAbs) against oxLDL has been shown to inhibit plaque development, possibly by facilitating the clearance of oxLDL [2].

The identification of high-risk vulnerable plaques represents a major clinical challenge [3]. The imaging modalities currently employed, such as intravascular ultrasound and optical coherence tomography, are invasive and mainly provide a measure of plaque burden and structure that does not directly translate to the risk

Table 1. Study design for digital autoradiography studies 1 and 2

Study	Animals (n)	Amount of mAb per injection		Injected activity of each tracer per animal				
		2D03 (μg)	Control mAb (μg)	^{131}I-2D03 (MBq)	^{125}I-control mAb (MBq)	^{125}I-2D03 (MBq)	^{131}I- control mAb (MBq)	^{18}F-FDG (MBq)
1	8	6.0	6.7	1.5	0.5	-	-	15
2	4	14.1	6.0	-	-	0.7	1.8	45

of a fatal clinical event [4]. Ongoing preclinical and clinical trials of additional imaging methods include magnetic resonance imaging and molecular imaging targeting, for example, inflammation and cell death using a variety of imaging modalities [4-6]. Animal studies and clinical trials using 2-deoxy-2-[^{18}F]fluoro-D-glucose (^{18}F-FDG) PET have shown a correlation of ^{18}F-FDG uptake with the presence of macrophages but not consistently with plaque vulnerability [5]. In this study we use 2D03, a human recombinant anti-oxLDL antibody specific to malondialdehyde (MDA) modified ApoB-100 protein [2], a natural occurring oxidation product known to be immunogenic in man [7].

Autoradiography, either of the whole aorta from an experimental animal or of transverse sections of the same aorta, is a common technique for evaluating potential imaging tracers [8-11]. Most, but not all [12], studies image only one single radiolabelled tracer per animal. The aim of this study was to use multi-radionuclide digital autoradiography with a real-time solid state detector to simultaneously compare the distribution of ^{18}F-FDG and ^{131}I/^{125}I labeled anti-oxLDL and control antibodies in an atherosclerotic mouse model.

Materials and methods

Human recombinant antibodies

Two recombinant human IgG1, lambda antibodies 2D03 and FITC8 were used. The 2D03 was produced as previously described [2]. An antibody binding to fluorescein isothiocyanate, FITC-8 (Bioinvent, Lund, Sweden), was used as a negative control.

Animal model

Male apoB-100/LDL receptor deficient mice with C57BL/6 background (B6; 129S-*Apob^{tm2Sgy}LDLr^{tm1Her}*/J; Jackson Laboratories, Bar Harbor, Maine), which express full length apoB-100 in their LDL particles were used. The mice were fed a high fat diet (0.15% cholesterol, 21% fat, Lantmännen, Stockholm, Sweden) from 4 weeks of age, provided *ad libitum*. All experiments were conducted in compliance with Swedish legislation on animal protection, and were approved by the regional ethics committee on animal experiments.

Digital autoradiography of specific, unspecific antibody, and ^{18}F-FDG

The specific 2D03 mAb and the nonbinding control mAb were radio-iodinated (both isotopes from MAP Medical Technologies, Tikkakoski, Finland) using the iodogen method [13]. In Study 1, 2D03 was labeled with ^{131}I ($T_{½}$ = 8.02 days, β^- and γ emitter) and the control mAb with ^{125}I ($T_{½}$ = 59.4 days, conversion e^-, γ and X-ray emitter) while for study 2, 2D03 was labeled with ^{125}I and the control mAb with ^{131}I. Radiolabelling efficiency was approximately 80-90%, measured by paper chromatography.

Atherosclerotic mice, 25 weeks of age, were injected intravenously with a mixture of both mAbs, as detailed in **Table 1**. Based on Study 1 results, the amount of 2D03 mAb was doubled in Study 2 in order to increase the amount of radioactivity in the aorta and improve the digital autoradiography image statistics. After 67 h post injection (p.i.) food was removed and by approximately 72 h p.i. animals were injected intravenously with ^{18}F-FDG (^{18}F: $T_{½}$ = 1.83 hours, β^+ emitter) and sacrificed one hour later. ^{18}F-FDG with radiochemical purity >99% was produced at Skåne University Hospital (Lund, Sweden). The mice were killed by intraperitoneal injection of 300 μl of a mixture of phosphate buffered saline (0.15M PBS pH 7.4, HyClone, Thermo Scientific, South Logan, Utah, USA), Xylazine (Rompun, Bayer Health care, Leverkusen, Germany) and Ketamine (Ketalar, Pfizer, New York, NY, USA), 3:1:1 vol/vol/vol and exsanguinated by cardiac puncture. Blood samples were taken on sacrifice and the activity was measured after ^{18}F decay in a NaI(Tl) well counter (Wallac Wizard 1480, PerkinElmer,

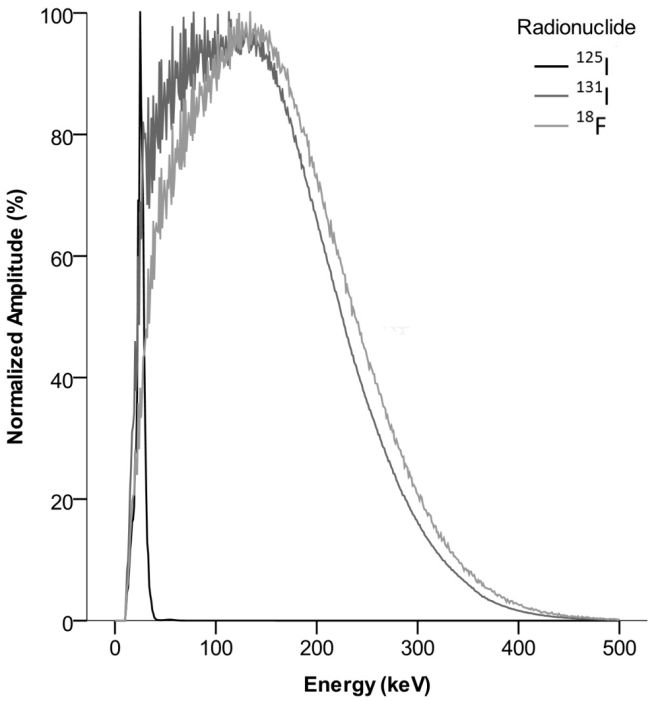

Figure 1. Individually normalized energy spectra for the radionuclides employed in this study as measured on the silicon strip digital autoradiography system. Note the similarity between the beta emitters ^{18}F and ^{131}I, whereas the conversion electron and x-ray peak for ^{125}I is very distinct.

Shelton, CT) capable of separating ^{125}I and ^{131}I. Next the animals were perfused with 5 mL PBS and then with 5 mL of the fixative Histochoice (Amresco, Solon, Ohio, USA). The descending aorta was dissected free of connective tissue and fat, cut longitudinally, and mounted *en face* lumen-side up on ovalbumin (Sigma-Aldrich, St. Louis, MO, USA) coated slides. The aortas were immediately imaged for a minimum of 1 hour each, using a double-sided silicon strip detector with an intrinsic spatial resolution of 50 μm (Biomolex 700 Imager, Biomolex, Oslo, Norway). After decay of ^{18}F each aorta was imaged again for at least 8 hours.

Separation of the contributions from each radionuclide to the autoradiography image

All data from imaging was stored in list-mode format and were analyzed using IDL 6.4 software (ITT Visual Information Solutions, Boulder, CO, USA). For both studies, the coordinates and deposited energy of all detected events during imaging were recorded and the time stamps of the moment of detection were also recorded for study 2.

Energy spectra for a pure sample of each radionuclide were acquired (**Figure 1**). In both studies, data in the second imaging session was used to separate ^{125}I and ^{131}I by best fit of these spectra to binned energy data in each pixel as previously outlined in Örbom et al 2007 [14]. To separate ^{18}F, reconstructed images of the ^{125}I and ^{131}I distributions, corrected for dead or miscalibrated strips and smoothed by a 5x5-pixel mean filter, were subtracted from the image containing all events in the first imaging session. The amplitude of the images to be subtracted was determined by using the ^{125}I peak in the energy spectrum as a reference for study 1 and correcting for radionuclide decay and differing imaging duration. For study 2, an energy threshold of 40 keV was used to exclude ^{125}I and then ^{18}F and ^{131}I were separated by the rate of decay using best fit to time-binned data.

Immunohistochemistry (IHC)

Two 25 weeks old apoB-100/LDLr$^{-/-}$ mice were intravenously injected with 2 mg/kg dose of unlabeled 2D03 or control antibody. After 72 hours the animals were sacrificed and the aortas were removed, cleaned from fatty tissue and snap-frozen in liquid nitrogen. Aortas were sectioned into 4 μm thick consecutive sections, dried overnight and fixed with 100% ice-cold acetone. Before staining sections were rehydrated in Tris–HCl, pH 7.0, buffer containing 10% fetal calf serum. Macrophages were detected with anti-MOMA (Abdserotec, Oxford, UK) and oxLDL with the 2D03 antibody. Anti-human Ig or anti-mouse Ig Vectastain ABC kit (Vector Laboratories, Burlingame, CA, USA) was used as secondary reagents.

Plaque to aorta contrast

After imaging, the aortas were stored in Histochoice and later washed in distilled water, dipped in 78% methanol, and stained for 40 minutes in 0.2% Oil Red O dissolved in 78% methanol/0.2 mol/L NaOH as previously described [15]. Oil Red O stains lipids red, which makes the plaques bordeaux colored. The cover slides were mounted with a water soluble mounting media L-550A (Histolab, Göteborg, Sweden) and the aortas imaged

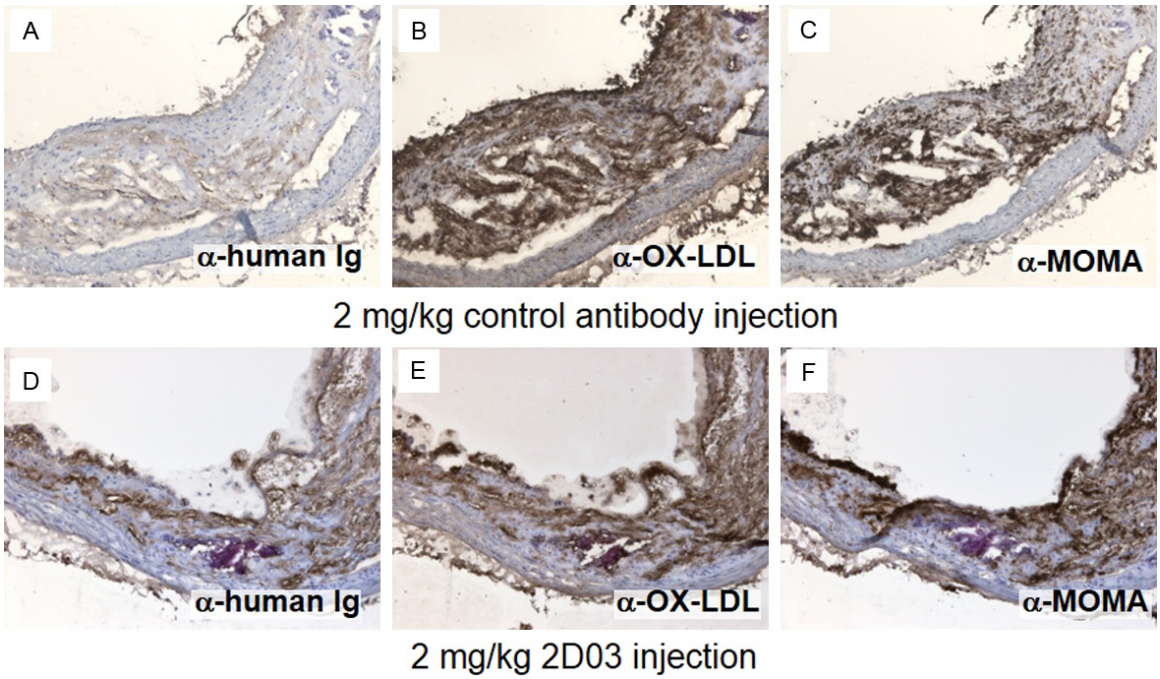

Figure 2. Immunohistochemical staining of consecutive sections of aortic plaques from mice injected with control antibody (A-C) and with 2D03 antibody (D-F). In (A and D), the sections were stained with a secondary anti human IgG to visualize endogenously present antibody. Sections in (B and E) are both stained in vitro with additional 2D03 antibody to visualize the total available 2D03 epitopes. In (C and F), the sections are stained for macrophages (anti-MOMA).

using a light-microscope slide scanner (Mirax Midi, Carl Zeiss, Oberkochen, Germany). Regions of the aorta were defined as containing either plaques or aorta wall based on staining intensity levels in the images as determined by visual inspection for each study. Images of the activity distribution of each radionuclide were registered to the plaque distribution images using numerical Powell optimization [16] of rigid transformations with a least-square error measure. For each activity distribution image, a ratio between the mean value of the registered counts in the regions containing plaques and the entire aortic wall was calculated.

Aorta antibody uptake

For study 2, the total activity of each iodine radionuclide in the excised aorta was also determined from the time-stamped digital autoradiography data. After correction for decay, the activities and sample weights were used to calculate percent injected activity per gram (%IA/g). The injected activities were determined by weighing syringes before and after injection.

Statistical analysis

The non-parametric related-samples Wilcoxon signed rank test was used to compare the plaque to aorta uptake ratios of ^{18}F-FDG with 2D03, ^{18}F-FDG with control mAb and 2D03 with control mAb, separately for both studies. The differences in uptake between control mAb and 2D03 in excised aortas (Study 2) were tested in the same manner. Tests were performed using IBM SPSS Statistics version 19 (SPSS, Chicago, IL, USA) with $p<0.05$ being considered significant.

Results

Immunohistochemistry

Frozen tissue sections from animals injected with high doses of unlabeled 2D03 or control antibody were analyzed for the presence of injected human antibodies and macrophages. The analyzed plaque showed an increased staining of human antibody in plaque from animals injected with 2D03 compared to the control animal (**Figure 2A** and **2D**). Additional in vitro staining with 2D03 indicated the total

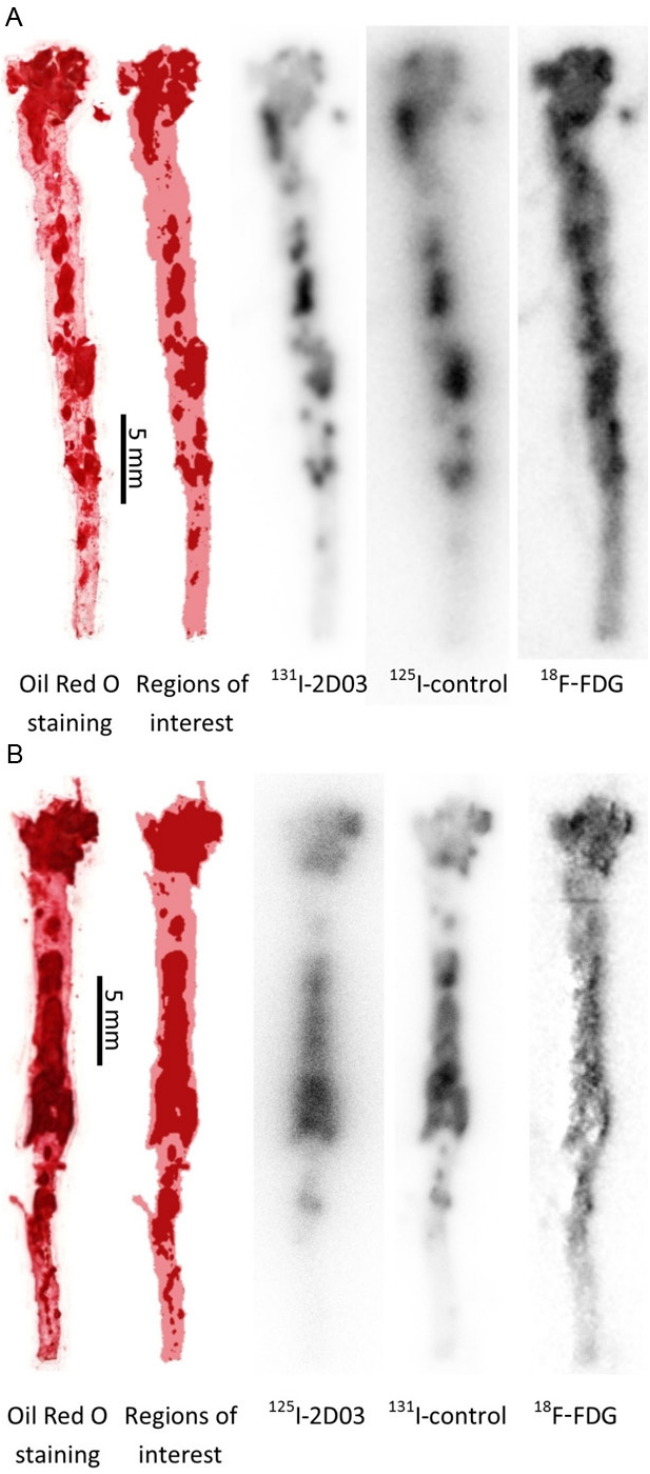

Figure 3. Images of the aorta from one animal from study 1 (A) and one from study 2 (B). From left to right, the aorta was stained with Oil Red O to identify the lipid deposits followed by the processed Oil Red O image to define plaque and non-plaque areas. Finally, with a 5x5-pixel mean filter applied, digital autoradiography images of the same aorta, separated into contributions from the different radiotracers. Each aorta is individually scaled from zero (white) to max (black) uptake and does not reflect differences in total uptake between different tracers.

overall presence of epitopes in 2D03 and control antibody injected animals (**Figure 2B** and **2C**) Illustrating the presence of additional epitopes in the lesions not targeted by this dose of antibody. Additionally, 2D03 showed localization to macrophage-rich areas in atherosclerotic plaques (**Figure 2E** and **2F**). Indicating a specific localization of 2D03 to the macrophage rich parts of the plaque.

Activity uptake relative to plaque distribution

As illustrated in **Figure 3**, Oil Red O staining revealed a heavy plaque burden along the whole length of the excised aortas in all animals with especially large and intensely stained areas directly below the aortic arch. Uptake of 2D03 and control mAbs were overall very similar irrespective of radionuclide, with a low uptake in the aortic wall but significant uptake in plaques. ^{18}F-FDG uptake was also observed in plaques, similar but not identical to the antibody uptake and with a higher uptake in the aortic wall. In the area directly below the aortic arch differences between antibody and ^{18}F-FDG uptake were common, revealing hotspots in different part of the plaques.

Plaque to aorta contrast

The plaque-to-aorta radionuclide uptake contrast (**Figure 4A**) was highest for the 2D03 antibody in both studies, irrespectively of the tracer or amount of antibody used. The median (range) ratios were 2.2 (1.9-2.6) for ^{131}I-2D03 compared to 1.6 (1.4-1.8) for ^{18}F-FDG and 1.7 (1.6-2.0) for ^{125}I-control mAb in study 1. The median (range) ratios in study 2 were 2.4 (1.8-2.9) for ^{125}I-2D03 versus 1.8 (1.2-2.0) for ^{18}F-FDG and 2.0 (1.7-2.2) for ^{131}I-control mAb. The differences in contrast between tracers when tested pairwise were found to be statistically significant between all possible pairs for study 1 (^{18}F-FDG:2D03 $p = 0.012$, ^{18}F-FDG:control $p = 0.036$, 2D03:control $p = 0.012$) but not for study 2 (^{18}F-FDG:2D03 $p = 0.068$, ^{18}F-FDG:control $p = 0.068$, 2D03:control $p = 0.068$).

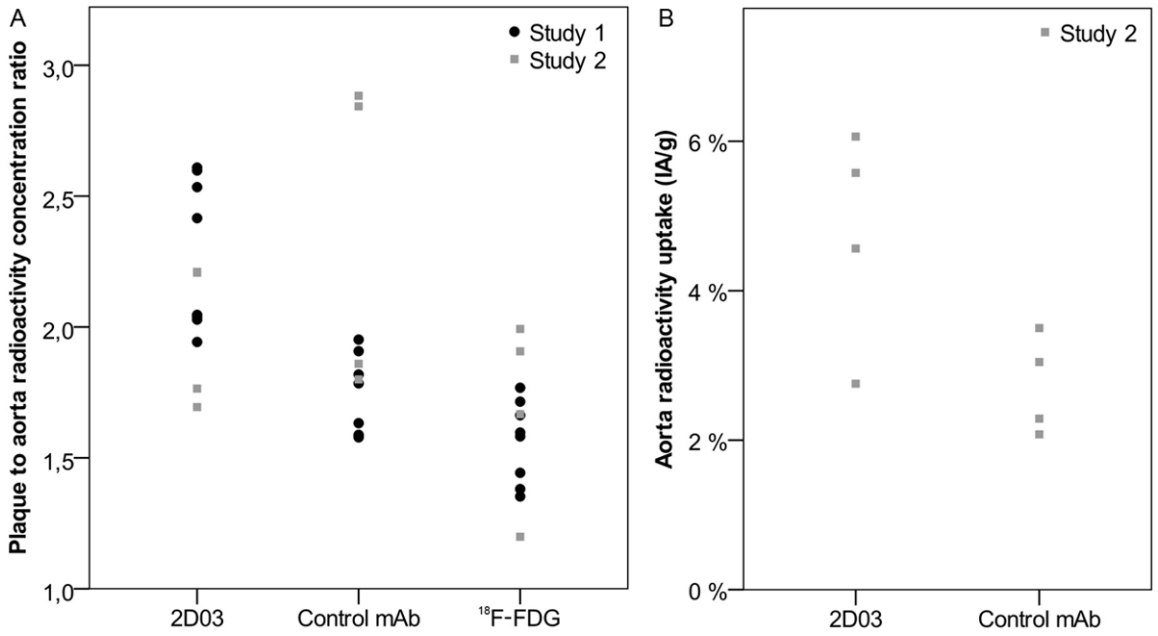

Figure 4. The plaque to aorta radioactivity concentration ratio as determined by dividing the mean image intensity in areas of autoradiography images defined as plaques by that of areas defined as aorta wall for each separated radionuclide image and each animal in both studies (A). And the total specific activity in the mounted aortas as determined by quantified autoradiography images of ^{125}I-labelled 2D03 and ^{131}I-labelled control antibody for study 2 (B).

Aorta antibody uptake

In study 2 we measured the median (range) fraction of activity in the excised aortas, which was higher for ^{125}I-2D03 compared to ^{131}I-control antibody at 5.1 (2.8-6.1) %IA/g versus 2.7 (2.1-3.5) %IA/g, respectively (**Figure 4B**). The difference in uptake between the tracers was however not found to be statistically significant ($p = 0.068$).

Blood activity

The median (range) fraction of activity in blood at the moment of sacrifice was measured for the antibodies, the results showed a high degree of variability at 4.3 (1.2-4.7) %IA/g for ^{131}I-2D03 and 4.6 (4.3-5.2) %IA/g for ^{125}I-control mAb for study 1 and 1.6 (0.9-2.2) %IA/g for ^{125}I-2D03 and 5.0 (2.4-5.3) %IA/g for ^{131}I-control mAb for study 2.

Discussion

This study demonstrates the imaging of three different radiotracers in atherosclerotic plaques *ex vivo* using a real-time digital autoradiography system. Both image analysis and measured plaque to aorta contrast indicate that the anti-oxLDL and the control antibody better differentiate between lesion and background in the excised and mounted mouse aorta than ^{18}F-FDG due to the apparent uptake of ^{18}F-FDG in the vessel wall. At the time point assayed we measured a higher, if not statistically significantly so, uptake of the 2D03 antibody in the aortas compared to the FITC-8 control. And the 2D03 antibody provided significantly higher plaque-to-aorta radionuclide uptake contrast compared both to control antibody and to ^{18}F-FDG. A high plaque-to-aorta ratio is necessary but not sufficient for a tracer to qualify as a candidate for future PET or SPECT diagnostic imaging and these results could form the basis for further research.

IHC showed weak staining for the control antibody, somewhat contrary to the autoradiography results though not unexpected since staining involves removal of any unbound antibody that may be present *in vivo*. Though the specific binding of 2D03 causes a higher amount to be accumulated, the overall distribution to atherosclerotic plaques rather than to the vessel wall may also be similar for any antibody due to trapping in the expanded surrounding of the inflamed aorta wall. A better result might be achieved by assaying the antibody uptake at

another time point, alternatively using a smaller more rapidly cleared antibody format such as a Fab fragment.

Autoradiography image analysis was confounded by differences in statistical noise between tracers due to fewer registered counts for ^{18}F. Additionally, there are differences in spatial resolution, due to the detector interacting with low energy x-rays emitted from ^{125}I, between the different radionuclides. For future studies, labeling the antibodies with e.g. ^{177}Lu and ^{111}In, using a DTPA conjugate, should produce more comparable images. For ^{18}F-FDG, either injected activity or imaging time could be increased. Since the animals did not receive any thyroid blocking compound, any free iodine released from the antibody should have been taken up by the thyroid and should not have introduced any artifacts in the intra-aortic activity distribution. Using whole mounted aortas has the benefit of showing many plaques in one single image, however the combined thickness of the aorta and the plaques may have introduced quantification errors. This could have been due to absorption as well as exaggerated uptake in plaques that will be found marginally closer to the detector surface thus affecting the resulting image [10].

Comparable studies largely differ both in animal models used and analysis methods employed and have, for example, found both similar [10] and higher [12, 17] values for plaque to aorta contrast for ^{18}F-FDG. For antibodies or smaller molecules against targets other than oxLDL, higher contrast ratios are generally reported, [11, 18] which apart from different uptake and clearance characteristics may be partly due to calculating from smaller regions of interest rather than the whole image. In a comparative study of several antibody derivatives injected into apolipoprotein E-deficient mice by Fiechter et al., the highest performing tracers generated autoradiography images visually similar to our results although different contrast ratios are reported [8].

To better evaluate the potential of the 2D03 antibody as a tracer for non-invasive imaging of vulnerable plaques, animal models developing such lesions could be used [19, 20]. Other time points and possibly smaller fragments of antibodies should also be explored since the relative long circulation time of an intact antibody will give a high background of nonbinding but lesion trapped labeled antibody. This might possibly explain the relatively high activity carried into the plaques by the non-specific FITC-8 control antibodies, despite a relatively weak presence of these antibodies into the lesions compared to 2D03, as determined by IHC. The high degree of variability seen in the activity in blood at the moment of sacrifice could be explained by the higher dose of 2D03 used in study 2. *In vivo* imaging using some combination of (multi-radionuclide) SPECT/CT and PET/CT will be included in further studies in order to find an optimal imaging time post injection and determine the biodistribution and pharmacokinetics of the tracers, e.g. the rate of tracer clearance from blood. While other imaging techniques such as micro-autoradiography using photographic emulsion, or additional immunohistochemistry, can provide data at higher spatial resolutions than around 100 μm, the relative ease of use and multi-radionuclide capabilities of our method recommends it as an additional component of *in vivo* radionuclide imaging studies to determine the overall intra-aortic distribution of a tracer compared to one or more controls. Possible effects of simultaneous injections of several tracers in the case of multi-radionuclide imaging must however be controlled for and the additional image statistics required for radionuclide separation may often require either higher than usual injected activities or a lower throughput study design. The primary application of the multi-radionuclide autoradiography would be to simultaneously evaluate multiple radiopharmaceuticals in one single animal e.g comparing distribution patterns of different antibodies in the same animal or comparing the localization of antibodies with uptake of a small molecule. Optimally the technique could be used as a preclinical evaluation method for potential drug candidates. 2D03 bind a specific form of oxLDL a substance associated with deposition of LDL, fatty streaks and foam-cells in the artery. ^{18}F-FDG is already in use in the clinic as an indirect measurement of macrophage activity. Our preliminary results indicate that measuring the presence of Ox-LDL with a specific antibody doesn't coincide fully with the activity of macrophages, a result which was not obvious before the analysis.

Conclusions

Multi-radionuclide digital autoradiography can be employed to compare several tracers *ex vivo*

in the same animal; however, the choice of radionuclides will influence image quality. Iodine labeled anti-oxLDL antibodies seem to achieve a better plaque to aorta contrast compared to unspecific control antibodies at 72 h p.i. and to ^{18}F-FDG 1 h p.i. in the excised aorta of apoB-100/LDL receptor deficient mice. The oxLDL specific antibody was enriched in the atherosclerotic lesions but its intra-aortic distribution does not significantly differ from the distribution of the control antibody.

Acknowledgements

The authors would like to thank Ingrid Söderberg and Ming Zhao for practical assistance. We would also like to thank Håvard Hauge at Biomolex AS for his technical assistance with the system. Funding for this project was provided by the Eurostars program through the Swedish Governmental Agency for Innovation Systems (VINNOVA), the Swedish Medical Research Council, the Swedish Heart-Lung foundation and the Albert Påhlsson foundation.

Disclosure of conflict of interest

Bo Jansson is an employee of BioInvent AB.

Address correspondence to: Anders Örbom, Department of Medical Radiation Physics, Lund University, Barngatan 2:1, SE-22185 Lund, Sweden. Tel: +46 46 222 0839; Fax: +46 46 178 540; E-mail: anders.orbom@med.lu.se

References

[1] Libby P, Lichtman AH and Hansson GK. Immune effector mechanisms implicated in atherosclerosis: from mice to humans. Immunity 2013; 38: 1092-1104.

[2] Schiopu A, Frendeus B, Jansson B, Soderberg I, Ljungcrantz I, Araya Z, Shah PK, Carlsson R, Nilsson J and Fredrikson GN. Recombinant antibodies to an oxidized low-density lipoprotein epitope induce rapid regression of atherosclerosis in apobec-1$^{-/-}$/low-density lipoprotein receptor$^{-/-}$ mice. J Am Coll Cardiol 2007; 50: 2313-2318.

[3] Seneviratne A, Hulsmans M, Holvoet P and Monaco C. Biomechanical factors and macrophages in plaque stability. Cardiovasc Res 2013; 99: 284-293.

[4] Gallino A, Stuber M, Crea F, Falk E, Corti R, Lekakis J, Schwitter J, Camici P, Gaemperli O, Di Valentino M, Prior J, Garcia-Garcia HM, Vlachopoulos C, Cosentino F, Windecker S, Pedrazzini G, Conti R, Mach F, De Caterina R and Libby P. "*In vivo*" imaging of atherosclerosis. Atherosclerosis 2012; 224: 25-36.

[5] Kusters DH, Tegtmeier J, Schurgers LJ and Reutelingsperger CP. Molecular imaging to identify the vulnerable plaque--from basic research to clinical practice. Mol Imaging Biol 2012; 14: 523-533.

[6] Ripa RS, Knudsen A, Hag AM, Lebech AM, Loft A, Keller SH, Hansen AE, von Benzon E, Hojgaard L and Kjaer A. Feasibility of simultaneous PET/MR of the carotid artery: first clinical experience and comparison to PET/CT. Am J Nucl Med Mol Imaging 2013; 3: 361-371.

[7] Fredrikson GN, Schiopu A, Berglund G, Alm R, Shah PK and Nilsson J. Autoantibody against the amino acid sequence 661-680 in apo B-100 is associated with decreased carotid stenosis and cardiovascular events. Atherosclerosis 2007; 194: e188-192.

[8] Fiechter M, Frey K, Fugmann T, Kaufmann PA and Neri D. Comparative in vivo analysis of the atherosclerotic plaque targeting properties of eight human monoclonal antibodies. Atherosclerosis 2011; 214: 325-330.

[9] Nakamura I, Hasegawa K, Wada Y, Hirase T, Node K and Watanabe Y. Detection of early stage atherosclerotic plaques using PET and CT fusion imaging targeting P-selectin in low density lipoprotein receptor-deficient mice. Biochem Biophys Res Commun 2013; 433: 47-51.

[10] Zhao Y, Kuge Y, Zhao S, Morita K, Inubushi M, Strauss HW, Blankenberg FG and Tamaki N. Comparison of ^{99m}Tc-annexin A5 with ^{18}F-FDG for the detection of atherosclerosis in ApoE-/- mice. Eur J Nucl Med Mol Imaging 2007; 34: 1747-1755.

[11] von Lukowicz T, Silacci M, Wyss MT, Trachsel E, Lohmann C, Buck A, Luscher TF, Neri D and Matter CM. Human antibody against C domain of tenascin-C visualizes murine atherosclerotic plaques ex vivo. J Nucl Med 2007; 48: 582-587.

[12] Matter CM, Wyss MT, Meier P, Spath N, von Lukowicz T, Lohmann C, Weber B, Ramirez de Molina A, Lacal JC, Ametamey SM, von Schulthess GK, Luscher TF, Kaufmann PA and Buck A. ^{18}F-choline images murine atherosclerotic plaques ex vivo. Arterioscler Thromb Vasc Biol 2006; 26: 584-589.

[13] Salacinski PR, McLean C, Sykes JE, Clement-Jones VV and Lowry PJ. Iodination of proteins, glycoproteins, and peptides using a solid-phase oxidizing agent, 1,3,4,6-tetrachloro-3 alpha,6 alpha-diphenyl glycoluril (Iodogen). Anal Biochem 1981; 117: 136-146.

[14] Orbom A, Dahlbom M, Olafsen T, Wu AM and Strand SE. Serial digital autoradiography with

a silicon strip detector as a high resolution imaging modality for TRT dosimetry. IEEE Nucl Sci Symp Conf Rec 2007; 6: 4054-4056.

[15] Brånén L, Pettersson L, Lindholm M and Zaina S. A procedure for obtaining whole mount mouse aortas that allows atherosclerotic lesions to be quantified. Histochem J 2001; 33: 227-229.

[16] Powell MJ. A fast algorithm for nonlinearly constrained optimization calculations. Numerical analysis. Springer; 1978. pp: 144-157.

[17] Silvola JM, Saraste A, Laitinen I, Savisto N, Laine VJ, Heinonen SE, Yla-Herttuala S, Saukko P, Nuutila P, Roivainen A and Knuuti J. Effects of age, diet, and type 2 diabetes on the development and FDG uptake of atherosclerotic plaques. JACC Cardiovasc Imaging 2011; 4: 1294-1301.

[18] Laitinen I, Marjamaki P, Haaparanta M, Savisto N, Laine VJ, Soini SL, Wilson I, Leppanen P, Yla-Herttuala S, Roivainen A and Knuuti J. Non-specific binding of [^{18}F]FDG to calcifications in atherosclerotic plaques: experimental study of mouse and human arteries. Eur J Nucl Med Mol Imaging 2006; 33: 1461-1467.

[19] Najafi AH, Aghili N, Tilan JU, Andrews JA, Peng X, Lassance-Soares RM, Sood S, Alderman LO, Abe K and Li L. A new murine model of stress-induced complex atherosclerotic lesions. Dis Model Mech 2013; 6: 323-331.

[20] Millon A, Canet-Soulas E, Boussel L, Fayad Z and Douek P. Animal models of atherosclerosis and magnetic resonance imaging for monitoring plaque progression. Vascular 2013; [Epub ahead of print].